Models for Predicting the Pedestal at the Edge of H-mode Tokamak Plasmas

Arnold H. Kritz[1], Glenn Bateman[1], Alexei Y. Pankin[2], and Thawatchai Onjun[3]

[1] *Lehigh University, Bethlehem, PA, 18015, USA*

[2] *SAIC, San Diego, CA 92121, USA*

[3] *Sirindhorn International Institute of Technology, Thammasat University, Klong Luang, Pathumthani 12121, Thailand*

Two models, developed within integrated modelling codes to predict the height, width and shape of the pedestal at the edge of H-mode tokamak discharges and to predict the frequency of Edge Localized Modes (ELMs), are compared. One model was developed in the JETTO code [1,2] while the other model has evolved in the ASTRA code [3,4]. In both models, the steep gradient region of the pedestal is caused by a reduction of transport near the plasma edge and ELM crashes are triggered by MHD instabilities. For both models, compared in the Table below, the pedestal is included in the radial grid of the transport code.

	Model in JETTO Code	**Model in ASTRA Code**
Transport through pedestal:	Ion thermal neoclassical transport computed at top of pedestal for all channels of transport	Flow shear stabilization of ITG/TEM and resistive ballooning modes + ETG + neoclassical ion transport
Width of pedestal:	Prescribed width or scaling proportional to ion thermal Larmor radius	Width determined self-consistently from flow shear stabilization
ELM trigger:	MHD instability calibrated using HELENA and MISHKA MHD codes	MHD instability. Recently, trigger model developed using BALOO, ELITE, & DCON
ELM crash:	Thermal transport transiently increased by factor of 300. Particle transport transiently increased by factor of 100.	Profiles changed abruptly between time steps using empirical energy loss scaling.

Transport and Pedestal Formation

In the model developed in the JETTO code, the ion thermal neoclassical transport computed at the top of the pedestal is used for all the channels of transport throughout the pedestal. Since the pedestal width is usually smaller than the ion banana width, there is a case to be made for using a non-local model for the transport. It is more difficult to justify the use of ion thermal neoclassical transport for the electron thermal transport. A recent study has included the effect of magnetic ripple on the transport through the pedestal [5].

The pedestal width in the JETTO model is prescribed as a numerical value or an empirical scaling. In simulations of discharges with different hydrogenic isotope mass, it was found that the pedestal width must increase with isotope mass in order to produce agreement with experimental data [6]. The JETTO model for the pedestal width, however, is not yet self-consistently computed with the transport model. Normally, the Mixed-Bohm/gyro-Bohm transport model is used for the core transport.

In the model developed in the ASTRA code, different modes of turbulent-driven transport are flow shear stabilized and the pedestal width is predicted by the model. Turbulence modes with different correlation lengths are flow shear stabilized at different rates [4]. It is found that most of the flow shear in the simulations is produced by the diamagnetic velocity and the neoclassical poloidal velocity, so that a self-consistent computation of the toroidal velocity is not essential. Also, it is found that the simulation results are not significantly affected by whether the flow shear stabilization completely eliminates or smoothly reduces each mode of transport. The effects of magnetic shear stabilization are included within the computation of the transport for each mode. For example, high magnetic shear stabilizes the ITG/TEM mode that is computed using the Weiland model.

The electron thermal transport is a key issue that is under investigation. In the current version of the model in the ASTRA code, electron thermal transport is computed using a quasi-linear model for the ETG mode [7] together with a threshold condition [8]. The model used for the electron thermal transport determines the ratio of the electron temperature to the ion temperature at the top of the pedestal. It is clear from the simulations that neoclassical transport alone is not correct. The combination of neoclassical ion thermal transport and ETG electron thermal transport produces a pedestal that is too narrow and too steep. The effect of the Paleoclassical model on electron thermal transport is currently being explored [9].

Model for ELM Cycles

Each ELM crash is triggered by an ideal MHD instability in the models currently used in both the JETTO and in the ASTRA code. The stability criteria for ballooning modes used in the JETTO code is calibrated by hand against results from the HELENA and MISHKA ideal MHD stability code, while the peeling mode is calculated using the model developed in Ref. [10]. The ELM model in the JETTO has been tested under various scans, such as gas puffing scan, triangularity scan, and power scan, and the JETTO code has been able to reproduce JET H-mode experiments within reasonable agreement.

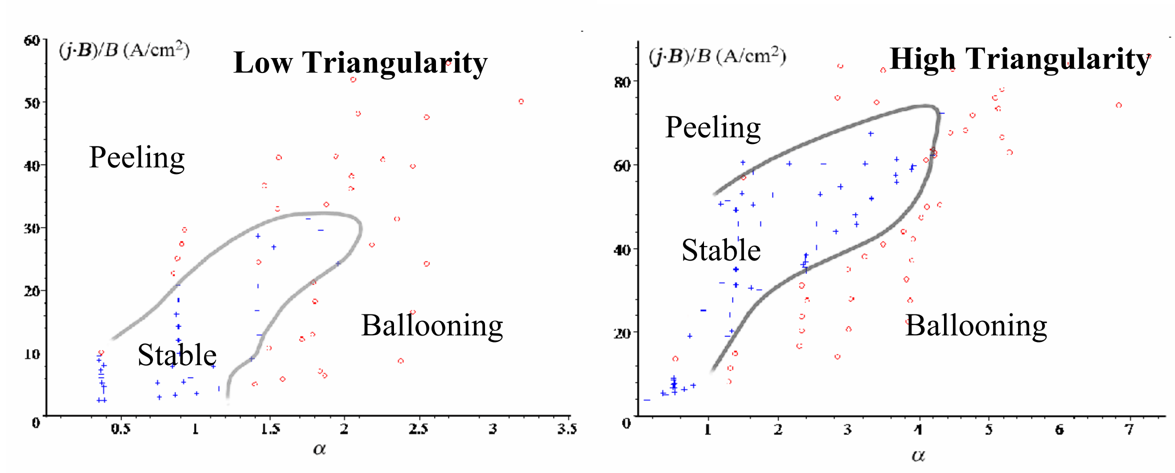

Fig. 1: MHD stability diagrams as a function of parallel current density, j·B/B, *and normalized pressure gradient,* α, *for low and high triangularity DIII-D equilibria.*

In recent ASTRA simulations, three ideal MHD stability codes (BALOO, ELITE, and DCON) were used to parameterize the ELM trigger model [11], as shown in Fig. 1. The BALOO code was used to compute the stability of high *n* modes, where *n* is the toroidal mode number. The ELITE code was used for intermediate and high *n* modes, and the DCON code was used for low *n* modes. The results for the stability criteria were parameterized with polynomial fits for DIII-D equilibria with low triangularity and high triangularity. The stability curves in Fig. 1 are plotted as a function of parallel current density, j·B/B, and normalized pressure gradient, α.

In simulations of discharges with sufficiently high heating power, ELM crashes limit the pressure gradient in the pedestal and, consequently, limit the peak pressure at the top of the pedestal. The frequency of the ELM crashes in the simulations increases with heating power, as it does for type I ELMs in experiments, and the numerical values of the ELM frequencies in the simulations are close the values observed in experiments. It is found that the stability region in parameter space becomes larger in high triangularity discharges, as shown in Fig. 1, in agreement with experimental data [2]. It is said that the pedestal plasma enters the second stability region of parameter space in high triangularity discharges. The peak pedestal pressure is roughly twice as high in the second stability region (the right hand panel in Fig. 1) than it would be in the first stability region (the left hand panel in Fig. 1). This second stability effect is found to produce favourable performance results in ITER simulations [12].

Different empirical ELM crash models are used in JETTO and ASTRA. In the JETTO model, the thermal transport in the pedestal is increased by a factor of 300 for about 0.5 msec, while the particle transport in the pedestal is increased by a factor of 100. In the model currently used in the ASTRA code, the temperature profiles are abruptly changed between time steps to produce a change in the plasma energy that is computed from an empirical scaling [4]. Since the loss of plasma energy during each ELM crash is an important issue, improved theory-based models are needed.

A major unresolved problem with the modelling of the ELM crash has to do with the current density that is removed from the pedestal by each ELM crash. The steep pressure gradient in the pedestal drives a relatively large bootstrap current density and, consequently, a relatively large current density that is localized to the pedestal toward the end of each ELM cycle. During each ELM crash, the pressure gradient in the pedestal is removed rapidly, but inductive effects slow down the removal of the current density. As a result, the current driven peeling and kink modes remain unstable after the initial stage of the ELM crash in the simulations and the ELM crash continues for a time that is much longer than the experimentally observed duration of the ELM crash [2]. One approach to resolving this problem is to reduce the current density and pressure gradient to the MHD marginal stability point, using the rationale that all of the free energy for driving MHD instabilities is removed.

Future Work

The best features of the pedestal and ELM models in the JETTO and ASTRA codes will be encapsulated in an NTCC module [13] for use in any suitable integrated modelling code. MHD stability codes are being used to generalize the parameterization of the ideal stability criterion that is used to trigger ELM crashes. Research has begun on a collaborative five-year edge fusion simulation project in which the formation of the pedestal will be simulated using 3-D non-linear gyro-kinetic codes and the ELM crash will be simulated using non-linear extended MHD instability codes. The objective of this project is to produce first principles simulations of ELM cycles, including the stabilization of turbulence and the computation of the remaining transport through the pedestal, the triggering of ELMs, and the subsequent non-linear evolution of ELM crashes.

Work supported by the Royal Thai Government and Development and Promotion for Science and Technology Talents Project and by U.S. DOE Contract No. DE-FG02-92-ER-5414.

1. V. Parail, *et al.,* Plasma Physics Reports **29** (2003) 539 ; J. Lönnroth *et al.,* Plasma Phys. Cont. Fusion **46** (2004) A249, 767 and 1197.
2. T. Onjun *et al.*, Phys. Plasmas **9**, 5018 (2002); **11** (2004) 1469 and 3006; **12** (2005) 012507.
3. G. Janeschitz, *et al.,* Plasma Phys. Control. Fusion **44** (2002) A459; G. Pacher *et al.,* Nucl. Fusion **43** (2003) 188.
4. A.Y. Pankin, *et al.,* Plasma Phys. Control. Fusion **47** (2005) 483.
5. J. Lönnroth *et al.*, 2005 Transport Task Force Meeting, Napa, CA and to be submitted for publication.
6. S. Snyder *et al., Effect of Isotope Mass in Simulations of JET H-Mode Discharges,* to be submitted.
7. W. Horton *et al.,* Phys. Plas. **7** (2000) 1494; M. Ottaviani *et al.,* Plas. Phys. Control. Fusion **39** (1997) 1461.
8. F. Jenko *et al.,* Phys. Plasmas **8** (2001) 4096; Phys. Plasmas **7** (2000) 1904.
9. J. D. Callen, Phys. Rev. Lett. **94** (2005) 055002; IAEA Fusion Energy Conf. (2004) IAEA-CN-116/1-1.
10. J. W. Connor *et al.,* Phys. Plasmas 5, (1998) 2687.
11. A.Y. Pankin *et al.,* Czech Journal of Physics **55** (2005) 367.
12. T. Onjun *et al.,* to appear in Phys. Plasmas (2005).
13. A.H. Kritz *et al.,* Computer Phys. Comm. **164** (2004) 108; http://w3.pppl.gov/NTCC.